Pediatr Radiol (2012) 42:1029–1046
DOI 10.1007/s00247-012-2410-6

REVIEW

Neuroimaging of ventriculoperitoneal shunt complications in children

Ahilan Sivaganesan · Rajesh Krishnamurthy · Deshdeepak Sahni · Chitra Viswanathan

Received: 2 September 2011 / Revised: 24 February 2012 / Accepted: 9 March 2012 / Published online: 28 June 2012

Abstract The ventriculoperitoneal shunt is the mainstay of treatment for hydrocephalus. Despite its widespread use and safety record, it often malfunctions due to complications such as obstruction, breakage, migration and infection. This necessitates a systematic approach to diagnosing the etiology of shunt failure. Any evaluation should begin with an appraisal of the patient's symptoms. In acute malfunction, nausea, vomiting, irritability, seizures, headache, lethargy, coma and stupor are seen. In chronic malfunction, neuropsychological signs, feeding pattern changes, developmental delay, decline in school performance, headaches and increased head size are often seen. The next step in evaluation is a CT scan of the head to evaluate ventricular size. Prior imaging studies should be obtained for comparison; if the ventricles have enlarged over time, shunt malfunction is likely. If there is no such increase or dilation in the first place, other diagnoses are possible. However, "slit ventricle syndrome" should also be considered. When prior imaging is not available, pumping the reservoir, a radionuclide shuntogram, a shunt tap or even surgical exploration are options. The goals of this paper are to provide an algorithm for evaluating shunt malfunction and to illustrate the radiographic findings associated with shunt failure.

Keywords Ventriculoperitoneal shunt · Hydrocephalus · Malfunction · Diagnosis · Children

CME activity This article has been selected as the CME activity for the current month. Please visit the SPR Web site at www.pedrad.org on the Education page and follow the instructions to complete this CME activity.

A. Sivaganesan
Baylor College of Medicine,
Houston, TX, USA

R. Krishnamurthy (✉)
EB Singleton Department of Pediatric Radiology,
Texas Children's Hospital,
6701 Fannin St., Suite 1280,
Houston, TX 77030, USA
e-mail: rxkrishn@texaschildren.org

D. Sahni
Department of Neurosurgery, Baylor College of Medicine,
Houston, TX, USA

C. Viswanathan
Department of Diagnostic Radiology, University of Texas MD Anderson Cancer Center,
Houston, TX, USA

Introduction

Hydrocephalus has a prevalence of approximately 0.5% in the United States, and accounts for 69,000 hospital admissions every year [1]. The traditional treatment for hydrocephalus is the placement of a valve-regulated V-P shunt. While it is effective and commonly used, there are considerable drawbacks. Shunts can fail due to a host of mechanisms including obstruction, breakage, migration and infection. This paper provides an overview of V-P shunts and alternative treatments for hydrocephalus, and discusses an algorithm for evaluating potential shunt failure. It then breaks down the causes of failure into well-defined categories based on clinical presentation, and provides radiographic examples of each entity.

Hydrocephalus

Hydrocephalus is the second most common congenital brain malformation [1]. The fundamental pathophysiology of hydrocephalus is an imbalance in the production and reabsorption rates of cerebrospinal fluid (CSF). Most cases involve impaired reabsorption, either due to obstruction of major CSF pathways (noncommunicating) or of the arachnoidal villi (communicating) (Table 1). CSF overproduction, however, is rare and is known to occur with choroid plexus tumors.

Treatment of hydrocephalus in children

The traditional treatment for hydrocephalus has been the placement of a valve-regulated ventricular shunt. These shunts usually terminate in the peritoneal cavity. In children with contraindications to a peritoneal shunt, the devices may terminate in the pleural cavity or right atrium of the heart. It is estimated that 30,000 CSF shunt procedures are performed every year in the United States [1], at a total cost of $94 million [2], and they have been responsible for a considerable reduction in morbidity and mortality related to hydrocephalus. Whereas the survival rate for treated hydrocephalus is now very high, in the 1950s before shunts were developed, 49% of patients died by the end of a 20-year observation period [3].

While remarkably well-engineered, there are disadvantages associated with ventricular shunts. The most prominent of these are the risks of infection, mechanical malfunction, obstruction and migration. If children remain shunt-dependent, there is certainly a need for shunt revision as well. Consequently, the overall viability of shunt function at 4 years is only 41% [4].

A few alternatives to VP shunt placement are available. In recent decades, endoscopic third ventriculostomy (ETV) has become a major intervention for children with obstructive hydrocephalus, with many centers reporting successful outcomes [5, 6]. A common indication for this procedure is uncomplicated noncommunicating hydrocephalus due to aqueductal stenosis or space-occupying lesions. ETV entails creating a hole in the floor of the third ventricle using a fiberoptic scope, which enables the free flow of intraventricular CSF to the subarachnoid space (Fig. 1). Studies now demonstrate that age is the main determinant of outcome post-ETV, with younger children, especially neonates, having a poorer prognosis [5]. Specifically, ETV resolves hydrocephalus in 80% of children older than 2 years of age, but is not as effective in children younger than 2 years due to immaturity of the arachnoid granulations [7]. Reduction in ventricular size following third ventriculostomy can be variable in onset and degree, and success of the procedure is best determined by CSF flow imaging using phase contrast MRI. Causes of failed third ventriculostomy include obstruction by Lillequist membrane, an arachnoid membrane extending from the dorsum sellae to the anterior edge of the mamillary body.

In some cases, a frontal ventricular catheter attached to a blind reservoir or Ommaya reservoir is left in place in case ETV fails and conversion to a VP shunt is necessary. Lumboperitoneal subarachnoid shunts are another alternative for treatment of communicating hydrocephalus and severe slit ventricle syndrome [8], but they have been associated with a shunt malfunction rate requiring revision in 8% of cases [9]. For children who are ineligible for these alternatives, or who have failed ETV, the treatment of choice is the insertion of a valve-regulated V-P shunt.

Anatomy of a V-P shunt

The V-P shunt consists of three parts: the proximal catheter, the reservoir/valve, and the distal catheter in the peritoneum. The catheters are typically made of silicon and have a diameter of 2–3 mm. They are hypointense on T1- and T2-weighted MRI images and hyperdense on CT. The reservoir and valve are typically radiolucent, but they have radiopaque markers to allow for visualization.

The proximal catheter is placed so that its tip is at the widest part of the lateral ventricle, away from the choroid plexus and anterior to the foramen of Monro, in the frontal horn. The catheter exits via a burr hole and connects to a reservoir that allows CSF fluid sampling and intraventricular pressure measurement. The reservoir connects to the inflow port of a one-way valve, while the distal catheter connects to the outflow port on the valve and is tunneled

Table 1 Classification of hydrocephalus

Type of hydrocephalus	Noncommunicating	Communicating
Location	Obstruction at ventricular level: foramen of Monro, aqueduct of Sylvius, fourth ventricle and its outflow tracts	Obstruction of CSF flow at arachnoid granulations
Causes	Tumors, cysts, inflammation, scarring, intraventricular hemorrhage, genetic disorders, congenital	Meningitis, trauma, intraventricular hemorrhage, subarachnoid hemorrhage

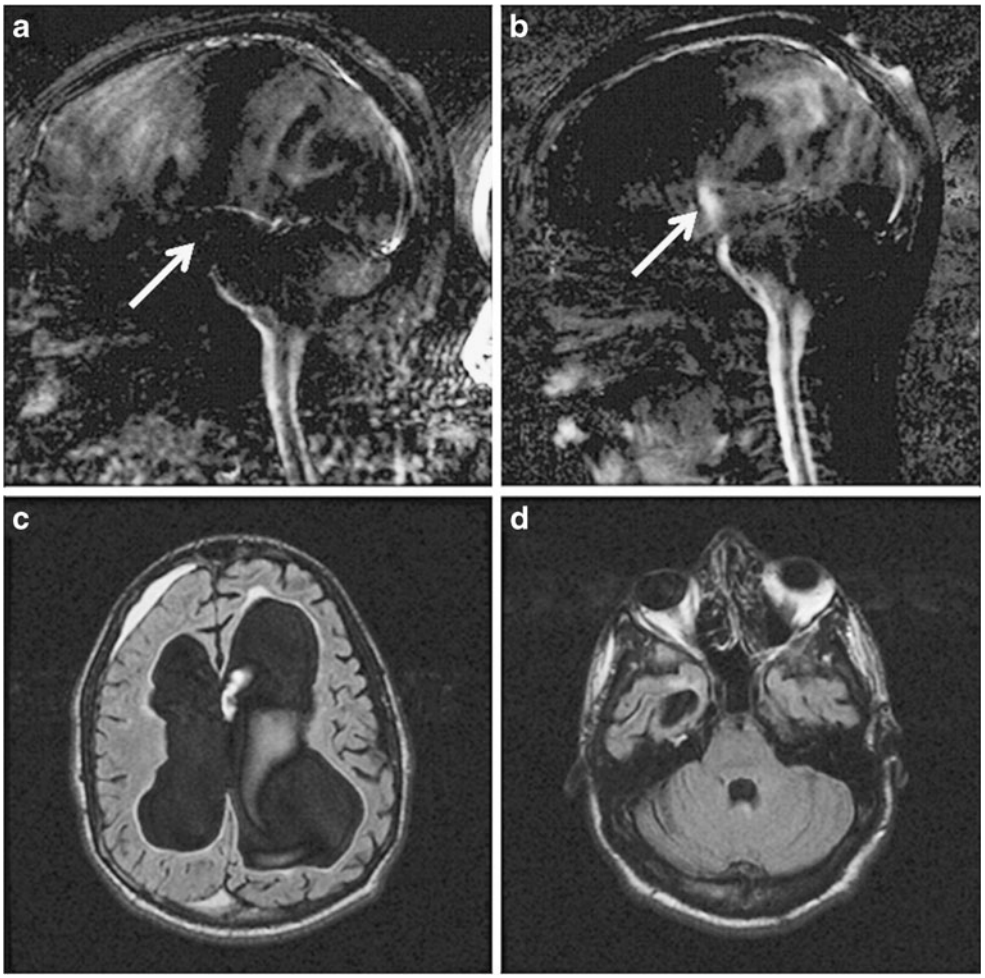

Fig. 1 Endoscopic third ventriculostomy. **a, b** Sagittal phase contrast images with superior-inferior flow encoding. Image (**a**) demonstrates lack of flow at the aqueductal level in a child with aqueductal stenosis (*arrow*) and (**b**), after endoscopic ventriculotomy (ETV), shows CSF flow in this location (*arrow*). **c** Axial FLAIR image from the same child shows lateral ventricular dilatation. **d** The 4th ventricle is small in comparison to the lateral ventricles, a presentation suggestive of triventriculomegaly due to obstruction of the aqueduct. This child is a particularly promising candidate for ETV

subcutaneously across the chest to terminate in the peritoneal cavity. The valve regulates CSF drainage, and plays an integral role in the successful treatment of hydrocephalus. The standard pressure differential valves can be divided into high-pressure systems and low-pressure systems on the basis of flow resistance. An important phenomenon that occurs with both types of valves is siphoning—the over-drainage of CSF due to increased pressure differentials between the proximal and distal catheters when a patient is standing. This over-drainage may lead to a negative intracranial pressure and collapse of the ventricles, but can be countered using anti-siphoning devices, flow-regulating valves, programmable valves and/or gravity-actuated valves.

Table 2 Postoperative findings after shunt placement

- Prompt or gradual decrease in ventricular size
- No change in ventricular size
- Ventricular collapse with mantle inversion
- Pneumocephalus
- Subarachnoid hemorrhage
- Intraventricular hemorrhage
- Parenchymal hemorrhage
- Subdural hematoma/hygroma

Fig. 2 Axial CT scan demonstrates acute hemorrhage in the right lateral ventricle in close proximity to the proximal catheter tip (*arrow*)

Fig. 3 Axial CT demonstrates cortical mantle inversion due to over-shunting (*white arrow*), with bilateral chronic subdural hematoma formation. There is also evidence of acute hemorrhage in the subdural space around the left frontal cortex (*curved white arrow*) and within the occipital horn of the right lateral ventricle (*black arrow*)

Programmable shunt valves, such as the Medtronic Strata Valve (Medtronic, Goleta, CA, USA) or Programmable Medos Valve (Codman/Johnson and Johnson, Raynham, MA, USA), allow the neurosurgeon to adjust the pressure within the ventricular space in an outpatient setting without having to revise the shunt in an operative setting [10].

Morphology of shunted ventricles

Obstructed ventricular systems have varying degrees of reduction in size following shunting, depending on the cause of hydrocephalus, its chronicity, and the presence of adhesions and loculations. A prompt reduction is expected in uncomplicated cases, with a CT scan 24 h after surgery showing a normal or slit-like appearance of the ventricles in 60–80% of shunted children [11]. In studies of children with spina bifida and hydrocephalus, cognitive function continued to improve when monitored 6 months after shunt placement [12]. Decrease in ventricular size following ETV, in contrast, may be more gradual and occur over several weeks.

CT findings in the postoperative period after shunt placement are listed in Table 2. One possible sequel to shunt placement or revision is intraventricular hemorrhage, which is a known predictor of future shunt failure (Fig. 2). In cases of hemorrhage, it is necessary to flush the ventricles to clear the clot, or insert a temporary drain until the hemorrhage clears. Another finding is ventricular collapse with mantle inversion, which may require the use of valves with increased flow resistance or anti-siphoning valves (Fig. 3). Two other possible findings are parenchymal hemorrhage, a rare complication with potential morbidity (Fig. 4), and subdural hematomas or hygromas, which usually follow a benign course (Fig. 5).

The problem of shunt malfunction

Suspected shunt malfunction is a frequent indication for emergent neuroimaging. Familiarity with the principles of shunt surgery, the natural history of ventricular shunts, clinical manifestations of shunt failure, and normal appearances and pitfalls of imaging are essential for prompt and accurate diagnosis of shunt malfunction. Pediatric studies have shown that shunt failures occur in 14% of children within the first month [13], and in up to 50% of children within the

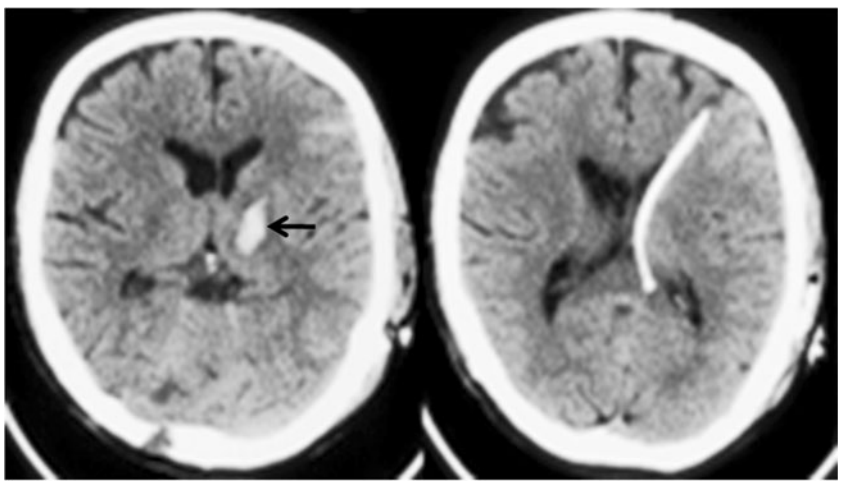

Fig. 4 Axial CT shows left-side thalamic hemorrhage (*arrow*) following proximal ventricular catheter placement

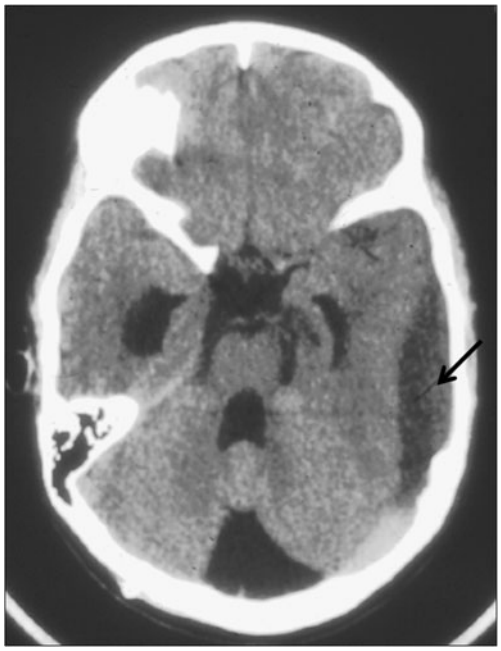

Fig. 5 Axial CT shows a left temporal chronic subdural hematoma following shunt placement (*arrow*)

first year [14]. Shunt revisions account for 48% of all shunt-related procedures performed in the United States [1].

Clinical manifestations of shunt malfunction

Shunt malfunction can manifest with a multitude of acute or chronic signs and symptoms (Table 3). For any given patient, however, every episode of shunt malfunction is characterized by a similar set of symptoms, making the clinical history an invaluable aid in diagnosing shunt failure. Studies of the predictive value of clinical signs and symptoms of shunt failure, within 5 months of placement, have borne this out [15]. The most notable signs and symptoms of shunt failure are nausea and vomiting (positive predictive value 79%), irritability (positive predictive value 78%), decreased level of consciousness (positive predictive value 100%) and a bulging fontanel (positive predictive value 92%) [15].

Table 3 Clinical manifestations of shunt malfunction

Acute	Subacute or chronic
Nausea	Change in behavior
Vomiting	Neuropsychological signs
Irritability	Change in feeding patterns
Seizures	Developmental delay
Headache	Change in school performance
Lethargy	Change in attention span
Coma	Daily headaches
Stupor	Increase in head size

Diagnosis of shunt malfunction

A universal cost-effective approach to evaluating suspected shunt malfunction is still elusive. Neurosurgeons, therefore, develop unique approaches to handling shunt malfunction based on their patient population, experiences and preferences. One survey of neurosurgeons revealed that they rely first on clinical history, then on change in ventricular size on CT, and finally on the shunt tap [16]. Examination of the shunt tract is also important, as a subgaleal collection near the reservoir may be the only sign of shunt failure. Another option, pumping of the reservoir by trained personnel, was long thought to yield valuable information about shunt malfunction, but it is now reported to be of little help in diagnosis and may, in fact, draw choroid plexus into the shunt [17].

In general, a multimodality approach is typically required for the diagnosis of shunt malfunction, with plain radiography, CT, radionuclide studies (shuntograms), MRI, CSF pressure studies and cultures providing complementary

Table 4 Steps in the evaluation of shunt malfunction

1) Medical history
   - Indication for shunt
   - Type of shunt
   - Dates of insertion and/or revision
   - History of shunt malfunction
   - Symptoms and signs associated with shunt malfunction (Table 3)
   - History of infection
2) Clinical examination
   - Complete neurological exam
   - Valve inspection
   - Shunt tract examination (fluid collection, disconnection)
3) Pumping the reservoir
   - Ease of compression (distal patency)
   - Rapidity of refill (proximal patency)
4) Imaging
   - CT of the head (compared with previous studies)
   - Radiographic shunt series
   - Radionuclide or contrast shuntogram
   - US of the abdomen
   - MRI of the head
5) Shunt tap
   - CSF pressure studies
   - Culture and sensitivity
6) Craniotomy and exploration
7) Shunt revision

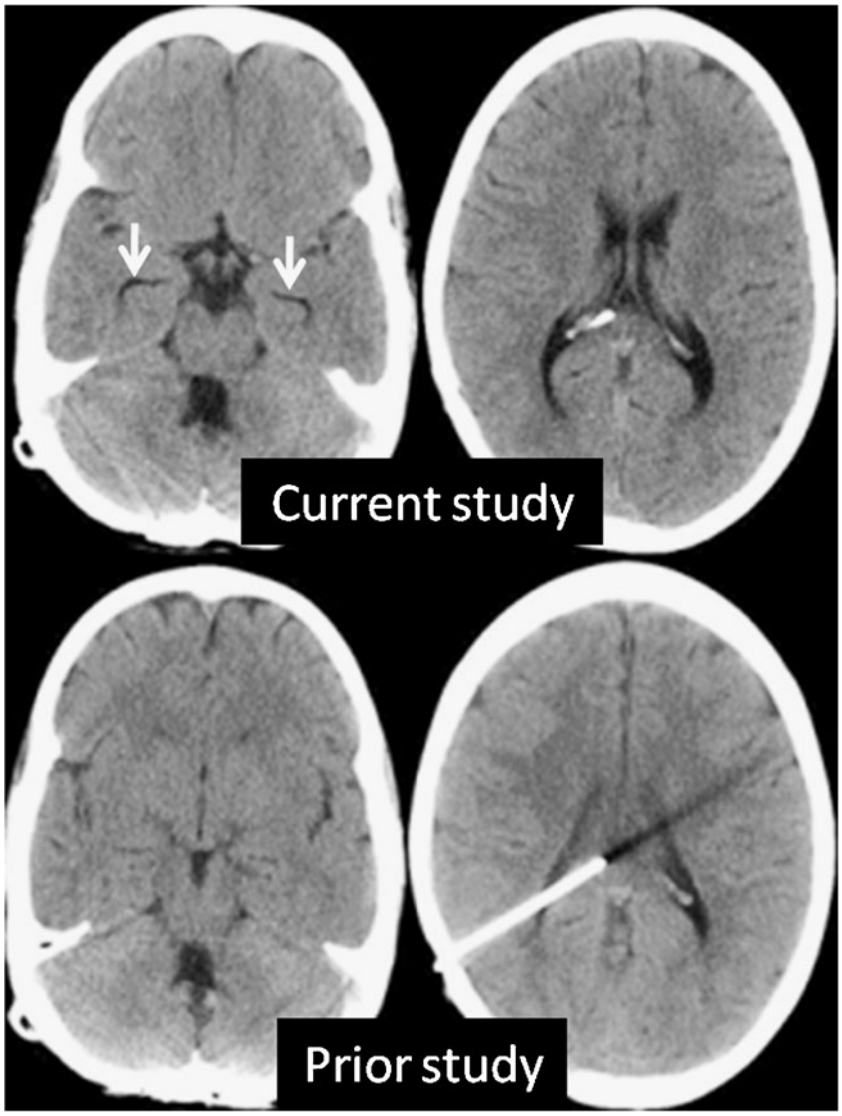

Fig. 6 Upper row: Axial CT demonstrates subtle temporal horn prominence (*arrows*) but relatively normal size of the body of the lateral ventricles. Lower row: comparison images from a prior CT from 1 month earlier shows collapsed ventricles. This represents a significant change, and is suggestive of acute shunt malfunction

information (Table 4). The standard unenhanced CT is the mainstay of diagnosis in the acute setting, providing information on ventricular size, shunt location, and the type and integrity of shunt components. A common problem in

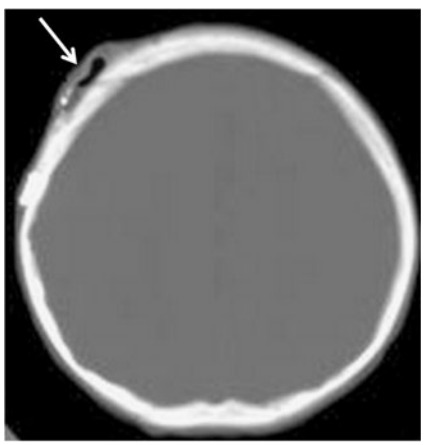

Fig. 7 Axial CT shows a collapsed shunt valve (*arrow*)

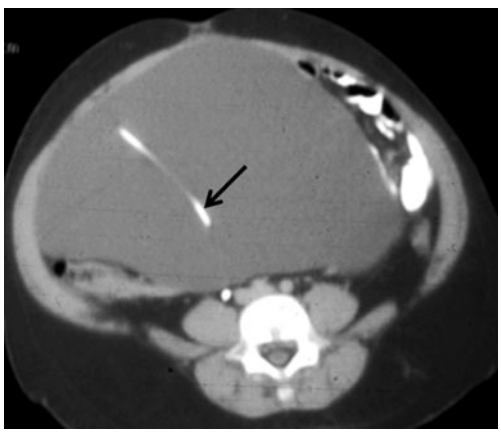

Fig. 8 Abdominal CT shows a large abdominal CSF pseudocyst. The distal shunt tip (*arrow*) terminates within the center of the pseudocyst

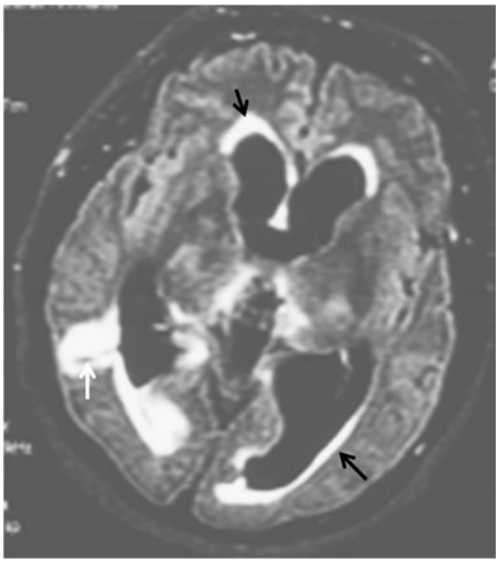

Fig. 9 Axial FLAIR demonstrates bilateral ventricular enlargement and transependymal flow of CSF (*black arrows*) along with peri-shunt edema in a child with acute shunt malfunction. The proximal catheter enters into the occipital horn of the right lateral ventricle (*white arrow*)

such acute settings, however, is lack of information about the child's baseline—head CTs are not routinely obtained when children are healthy. It is also important to avoid the assumption that the latest prior scan reflects the baseline, as it often represents the child's state after the onset of symptoms. Because these children may require multiple CTs for evaluation over their lifetime, it becomes prudent to adopt a low-dose CT protocol based on ALARA to decrease the effects of cumulative radiation, while maintaining image quality to accurately diagnose shunt malfunction. One series reports a 63% decrease in radiation dose by decreasing the mAs [18]. Another frequently used diagnostic option is the radiographic shunt series, but research suggests that it is not cost-effective as a primary tool for diagnosing shunt failure [19]. For children who initially present with swelling along the shunt tract, however, it is the investigation of choice. It is also indicated prior to shunt revision to localize the site of shunt failure. Alternatively, for children with a history of shunt malfunction, but unimpressive changes in ventricular size, shunt injection or radionuclide scans (shuntograms) are the preferable choice. Interestingly, the combination of CT and shuntogram has been shown to improve sensitivity of the diagnosis of shunt malfunction when compared to CT alone [20]. Another modality is MRI, which is

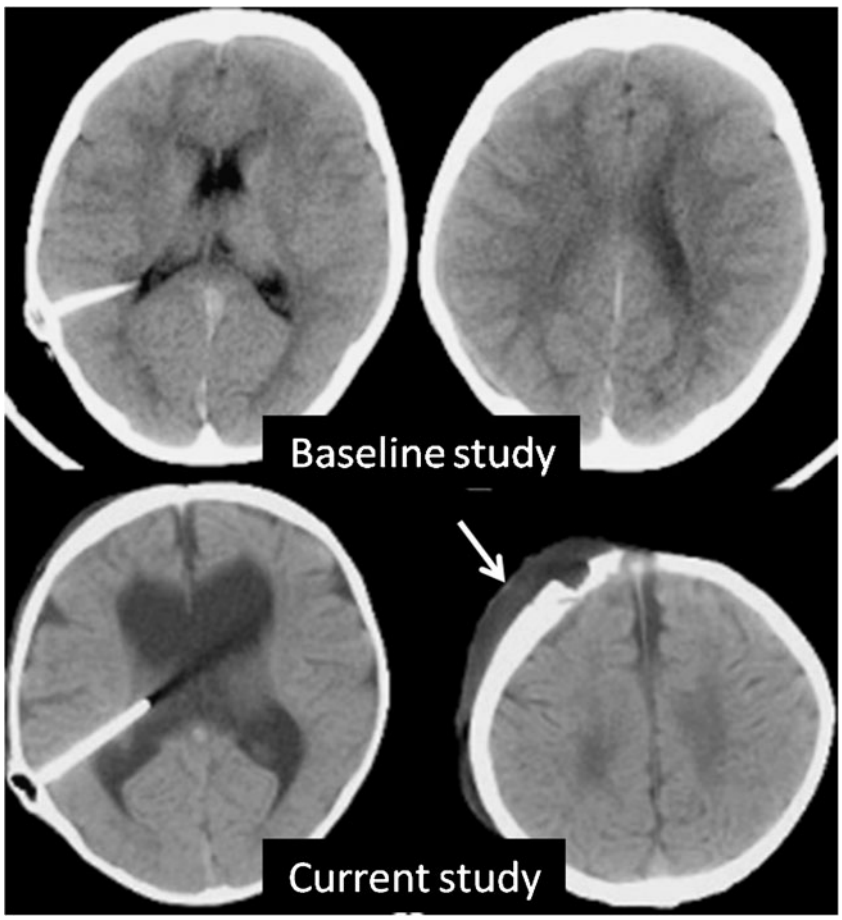

Fig. 10 Axial CT scans. Upper row: Baseline appearance of the ventricles and shunt. Lower row: Right-frontal subgaleal fluid (*arrow*) suggests shunt failure in the setting of ventricular enlargement

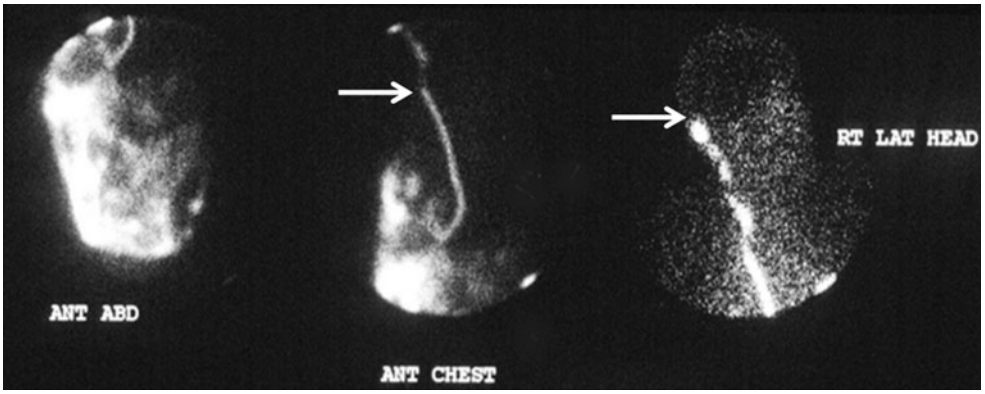

Fig. 11 Radionuclide shunt study demonstrates lack of contrast agent entry into the ventricular system (*arrows*) suggestive of proximal shunt obstruction. Contrast agent is noted to diffuse normally within the peritoneal cavity (left)

now being used more frequently, and has the potential to replace CT in the initial evaluation of shunt malfunction. Phase contrast imaging has been effectively used to determine patency and velocity of CSF flow in children with third ventriculostomies and shunts [21]. Single-shot fast spin-echo (SSFSE), or "quick brain" MRI, is as sensitive as CT in diagnosing shunt malfunction in the acute setting and does not expose children to radiation [22]. However, one must remember to re-evaluate the valve setting after MRI due to the possible effects of the magnetic field [10]. Finally, abdominal US can be used in settings where distal shunt obstruction due to pseudocyst formation or abscess is suspected. In these cases, one will see the shunt catheter within the pseudocyst.

Pathophysiology and imaging features of acute shunt malfunction

Obstruction

The clinical presentation of shunt obstruction varies with age. Infants often present with nausea, vomiting, irritability

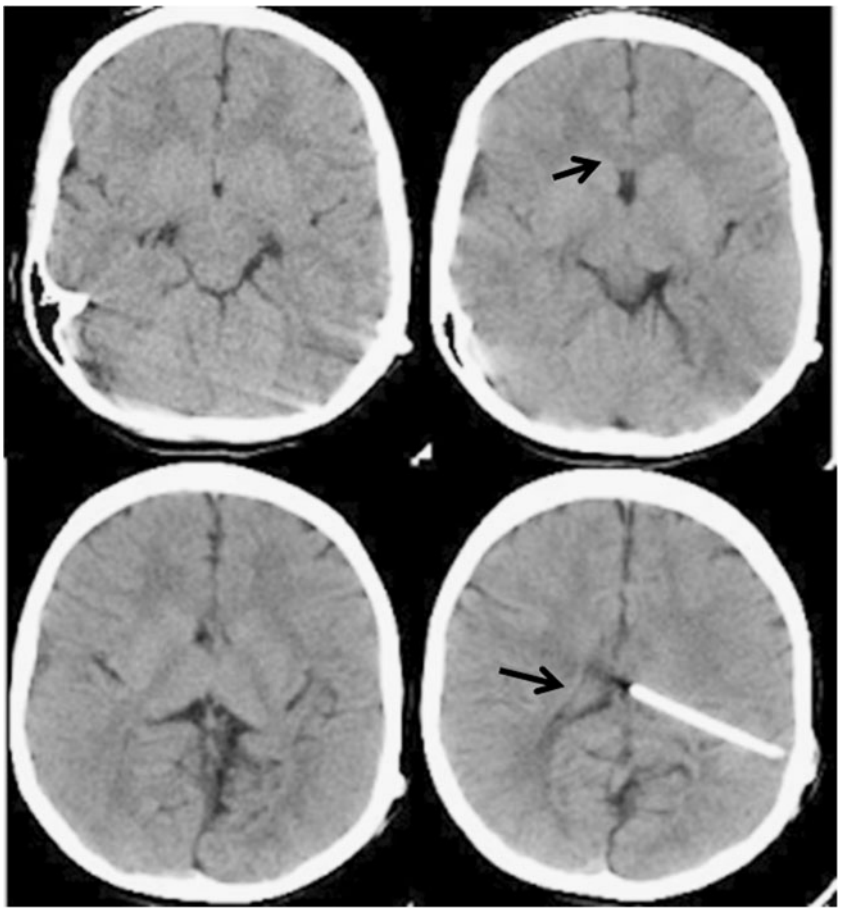

Fig. 12 Axial CT images show slit-like ventricles (*arrows*) in a child with shunt failure

Table 5 Slit ventricle syndrome subtypes

Clinical	Mechanism	Imaging	Diagnosis	Treatment
Postural headaches	Overdrainage of CSF due to negative intracranial pressure on standing	CT: subdural fluid collections, slit ventricles	ICP monitoring: negative pressures when upright	1. Valve pressure upgrade 2. Addition of second valve 3. Anti-siphon device insertion
"On-off again" symptom complex (Fig. 13)	Elevated CSF pressures despite functioning shunt. Related to reduced compliance of the ventricular walls to mild variations in CSF volume in chronically shunted patients with closed sutures.	CT: slit-like ventricles, manifestations of elevated CSF pressures in extracranial regions such as syrinx.	Intermittent increases in ICP with acute neurological changes	1. Shunt revision of no help 2. Medical treatment with Diamox or Lasix 3. Second-line rx with anti-migraine meds such as Inderal and Periactin 4. Cranial expansion is last resort
Recurrent obstructions of proximal catheter (Fig. 14)	Ventricular collapse around shunt resulting in shunt occlusion	CT: Contralateral ventricles enlarged (subtle or large) Previous CT scans useful	CT	1. Shunt revision and changing location of catheter tip 2. Valve pressure upgrade 3. Anti-siphon device
Subdural fluid collections (Fig. 15)	Result of compensated overdrainage of the ventricles	CT: Subdural fluid collection	CT	1. Subdural fluid collection external drainage 2. Shunt revision 3. Addition of anti-siphon device 4. Addition of higher-pressure valves

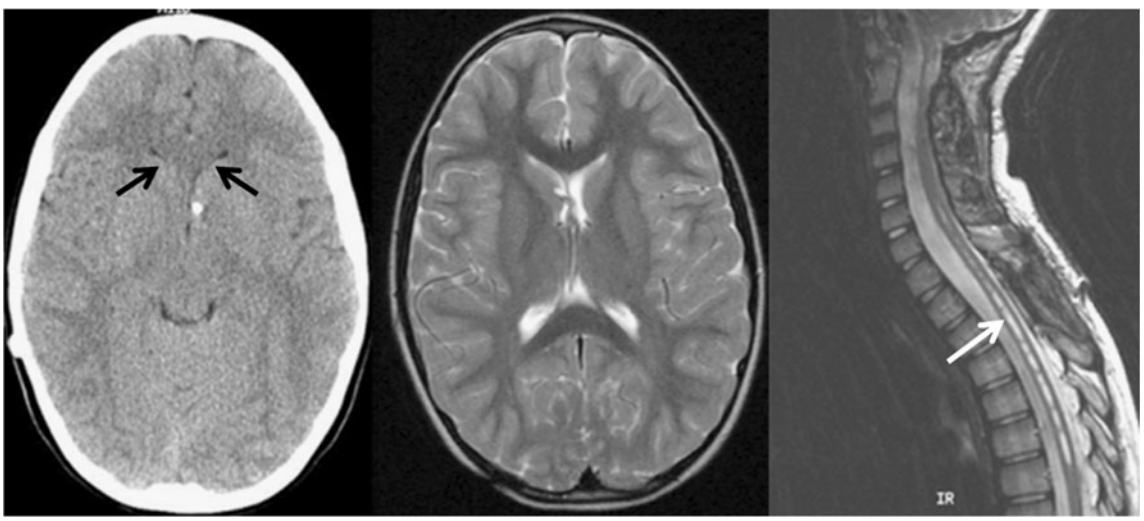

Fig. 13 CT and MRI show slit ventricles (*black arrows*) in a child with "on-off again" symptom complex, who also had a spinal cord syrinx extending from C6 to T7 (*white arrow*)

and a bulging fontanel. Older children and adults, however, present with symptoms such as headache, nausea, vomiting, cranial nerve palsies and ataxia [4]. A shunt can be occluded at three points: the proximal catheter, the valve and the distal catheter. The two most likely sites of obstruction are the ventricular catheter tip, which can be blocked by in-growing choroid plexus, and the shunt valve, which can be blocked by blood and debris [23]. Protein, brain parenchyma, ependymal cells, glial tissue, connective tissue and leptomeninges can also contribute to obstruction. In contrast to proximal blockages, which in one study accounted for 50% of all failures within two years of placement, distal blockages account for 14% of all failures [24]. Distal obstructions are often due to infection, CSF pseudocyst formation or catheter migration into the abdominal viscera. In general, the postoperative period has the highest risk of obstruction, due to debris, clots or catheter misplacement. The subsequent months have a progressively reduced risk, eventually approaching a constant 0.5% per month [25].

As stated above, the traditional bedside method of assessing shunt function by pumping the shunt reservoir is now known to have a low predictive value of 12% [26]. Radiographic imaging, on the other hand, is quite effective in assessing shunt function. Imaging can reveal a well-placed ventriculostomy tube, normal connections and ventricular enlargement. Comparison with pre-existing studies is critical for demonstrating signs of either overt or subtle ventricular enlargement (Fig. 6). In cases of proximal catheter obstruction, a collapsed reservoir may be seen on CT (Fig. 7). Alternatively, CT or US may show the CSF pseudocysts in the abdomen or pelvis (Fig. 8), and the latter modality is preferable due to the absence of radiation. When ventricular size is equivocal, blurring of the margins of the ventricles due to transependymal spread of CSF, peri-shunt edema (Fig. 9) and subgaleal fluid collections (Fig. 10) suggests the presence of acute obstruction. Furthermore, evaluation with radionuclide or contrast shuntograms, performed by injecting $^{99}Tc_m$—DTPA into a reservoir,

Fig. 14 Axial CT shows left lateral ventricular collapse (*arrow*) around the proximal catheter tip. This presentation can often result in shunt obstruction and clinical signs of failure

Fig. 15 Axial CT shows bilateral cortical mantle collapse (*arrows*) and mixed-density subdural hematoma formation due to overshunting

Fig. 16 Plain film with evidence of dystrophic calcification encircling the shunt tubing above the clavicle (*arrow*)

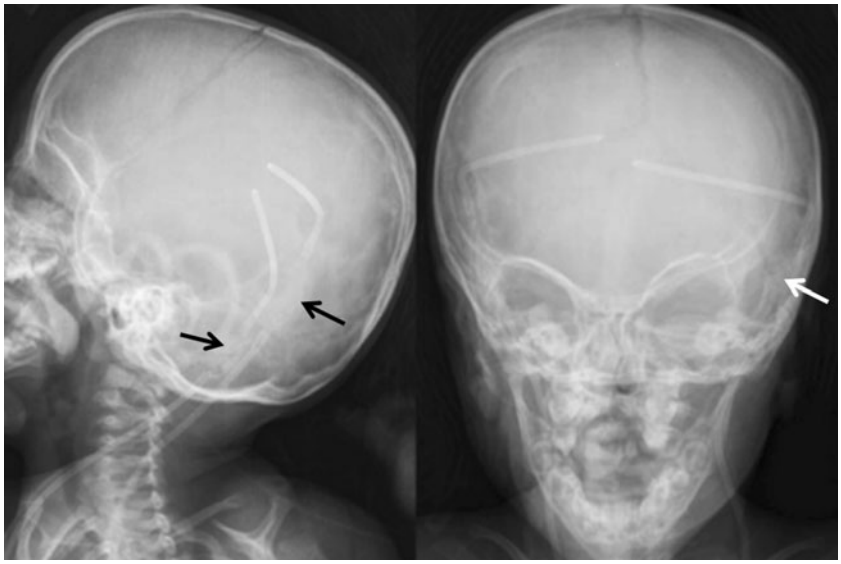

Fig. 17 Conventional radiograph of the skull shows radiolucent valves (*arrows*) that can appear to suggest shunt discontinuity

is useful for demonstrating obstruction in equivocal cases (Fig. 11). Studies in the past attributed high sensitivity and specificity to these shuntograms [27, 28]; however, a study in 2003 showed a false-negative rate of 14% [29].

Slit ventricles and slit ventricle syndrome

Nearly half of children with shunts may have small-size "slit-like" ventricles on CT [30–32]. However, up to 11% of children with symptoms of shunt failure can have slit-like ventricles as well, due to slit ventricle syndrome (SVS). SVS is not common, with various studies reporting an incidence less than 2%, but it is responsible for a disproportionate number of shunt revisions [33–35]. The surprisingly low incidence reported in the literature is possibly due to the late onset of SVS after shunt placement, as seen in one study that reported an average of 6.5 years prior to the onset of symptoms [36]. This explanation is corroborated by research that demonstrated a higher SVS incidence—10%—when follow-up was extended to 16 years [37]. SVS is hypothesized to be caused by either CSF overdrainage or by decreased compliance of the brain parenchyma to variations in CSF volume. Research suggests that 6–22% of children with radiological slit ventricles and headaches may have SVS due to this "non-compliant ventricle" syndrome [38,

Fig. 18 Shunt disconnection from the proximal catheter is seen on lateral and AP conventional radiographs (*arrows*). Axial CT on the right demonstrates ventricular enlargement

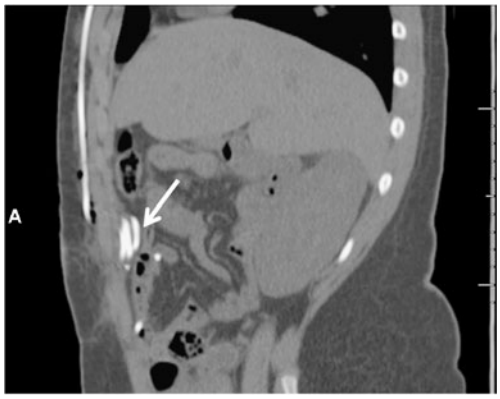

Fig. 19 Sagittal abdominal CT shows extraperitoneal placement of distal shunt catheter (*arrow*)

39] (Fig. 12). Four clinical entities of SVS—sometimes distinguishable using imaging—are recognized based on pathophysiology, and each requires different management (Table 5) (Fig. 13). Regardless of pathophysiology, however, children with a shunt placed before 1 year of age are uniformly at increased risk for SVS [40].

Apart from slit ventricle syndrome, less common manifestations of overshunting include lateral ventricular collapse around the proximal catheter tip (Fig. 14), or even cortical mantle collapse with subdural hematoma formation (Fig. 15).

Breakage

Shunt disconnection is the second most common cause of shunt failure in children [25], and it occurs most frequently in the neck region [41]. Factors predisposing to disconnection include increasing age of the shunt, restricted mobility, repetitive trauma, and the presence of catheter connections and valve junctions. As shunts age, they undergo calcification and biodegradation, making them more susceptible to breakage [25]. Fibrous tissue also develops along the length of the tubing, anchoring the catheter. Subsequent growth of the child then leads to shunt disconnection at the weakest link. It must also be noted that material failures, such as suture breakage, and surgical error are often primary causes of shunt disconnection [4].

One of the simplest investigations in diagnosing shunt breakage is palpating for fluid around the shunt tract; however, fibrous tissue tracts can be mistaken for a shunt catheter. Diagnoses of shunt disconnection are more often reached using a shunt series (AP/lateral skull, AP chest and KUB), which is the most sensitive diagnostic option [4], and a CT scan. A shunt series can reveal gaps between segments, which are radiolucent, and areas of calcification (Fig. 16). However, it is important to note that certain shunt components (Fig. 17) may also be radiolucent (valves, connectors and tubes) and should not be mistaken for disconnection —a common pitfall [42]. CT findings after shunt disconnection include subgaleal collections and enlarged ventricles (Fig. 18).

Malposition

Malposition of the proximal or distal limb of shunts can result in malfunction. Figure 19 shows one such error,

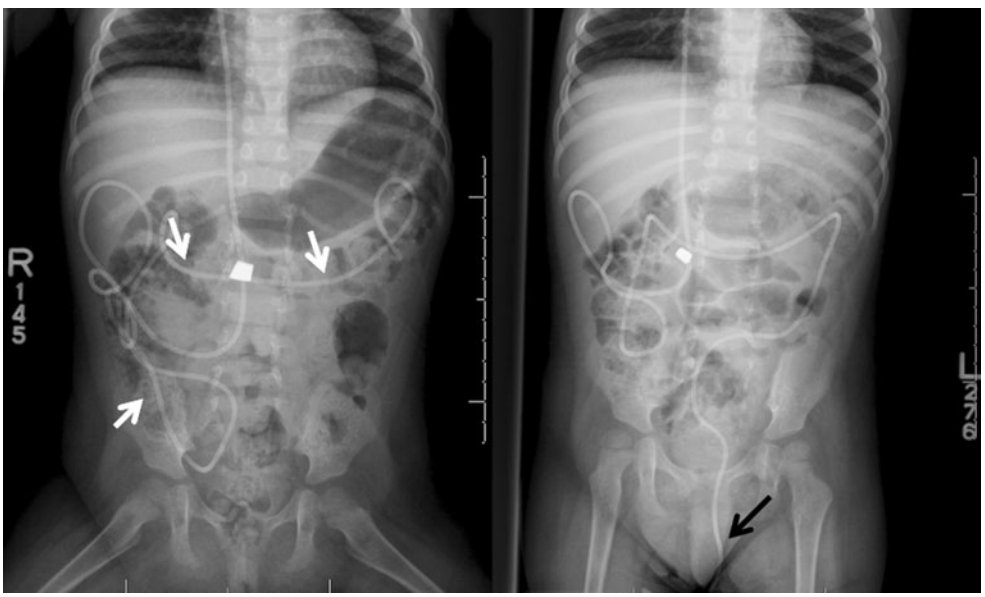

Fig. 20 Two examples of intracolonic migration of the catheter on abdominal radiographs. The clue to diagnosis is the course of the distal most portion of the shunt tube, which traces the path of the colon (*white arrows*). In the child on the right, the tip of the shunt catheter extrudes from the rectum (*black arrow*) (Image courtesy Dr. Amy Mehollin Ray, Texas Children's Hospital, Houston, TX)

Fig. 21 Abdominal plain film shows spontaneous knot formation of the distal shunt catheter (*arrow*)

in which the distal catheter has been placed in an extraperitoneal location. In certain cases, however, malfunction may not occur due to malposition if the lateral apertures of the catheter remain within the ventricle. This is especially true when the position of the shunt tip is unchanged from prior studies.

Migration

Shunt migration can occur at the distal or proximal end of the shunt. Once the catheter is fixed to the subcutaneous tissues by fibrous tissue, continued growth of the child results in traction and catheter migration. The proximal catheter can migrate to a nondraining area, such as the choroid, or to an extraventricular location in the parenchyma. Distally, extra lengths of tubing in the peritoneum for accommodation of future growth may result in migration of the tip into abdominal viscera, such as the colon, bladder, lung, rectum or scrotum. The risk of such migrations, research shows, is influenced by catheter type. Catheters with "snap" connectors form a strong 90° angle at the skull entry site and, therefore, are less likely to migrate. A minority of children with migration will experience a palpable change in shunt position and subsequent fluid collections around the shunt, but most of these diagnoses are made by imaging and not by physical exam [4]. Plain film or CT scan can show the extraperitoneal location (Fig. 20). In extremely rare circumstances, such migration of the distal catheter can lead to knot formation (Fig. 21).

Infection

Infection is a common cause of shunt failure, with an incidence of 8–10% according to multiple large trials. The majority of shunt infections occur within the first 6 months after surgery [4]. Intraoperative contamination by skin flora is the primary mode of infection, while other modes are proximal seeding from meningitis and distal seeding from peritonitis and wound infections [43, 44]. The signs of shunt infection are similar to the signs of shunt malfunction, namely nausea, headache and lethargy. Fever may or may not be present, so it is important not to exclude infection on this basis. Meningeal symptoms may also be absent because there is little communication between the infected ventricles and meningeal CSF. In most cases, the causative organism is *Staphylococcus epidermidis* (50%), with the remainder caused by *Staphylococcus aureus* (20%), gram-negative rods (15%) and *Propionibacterium acnes*. While lumbar puncture and ventricular punctures are routinely performed to attempt isolation of these bacteria, cultures are usually sterile. Instead, it is the shunt reservoir that typically allows for isolation of the organism. Imaging studies are typically not diagnostic in cases of infection, although ventriculitis may be seen on contrast-enhanced CT or MRI imaging as irregular enhancement of the

Fig. 22 Bilateral enhancement of the ependyma of the lateral ventricles on a T1-W postcontrast axial MRI (*arrows*)

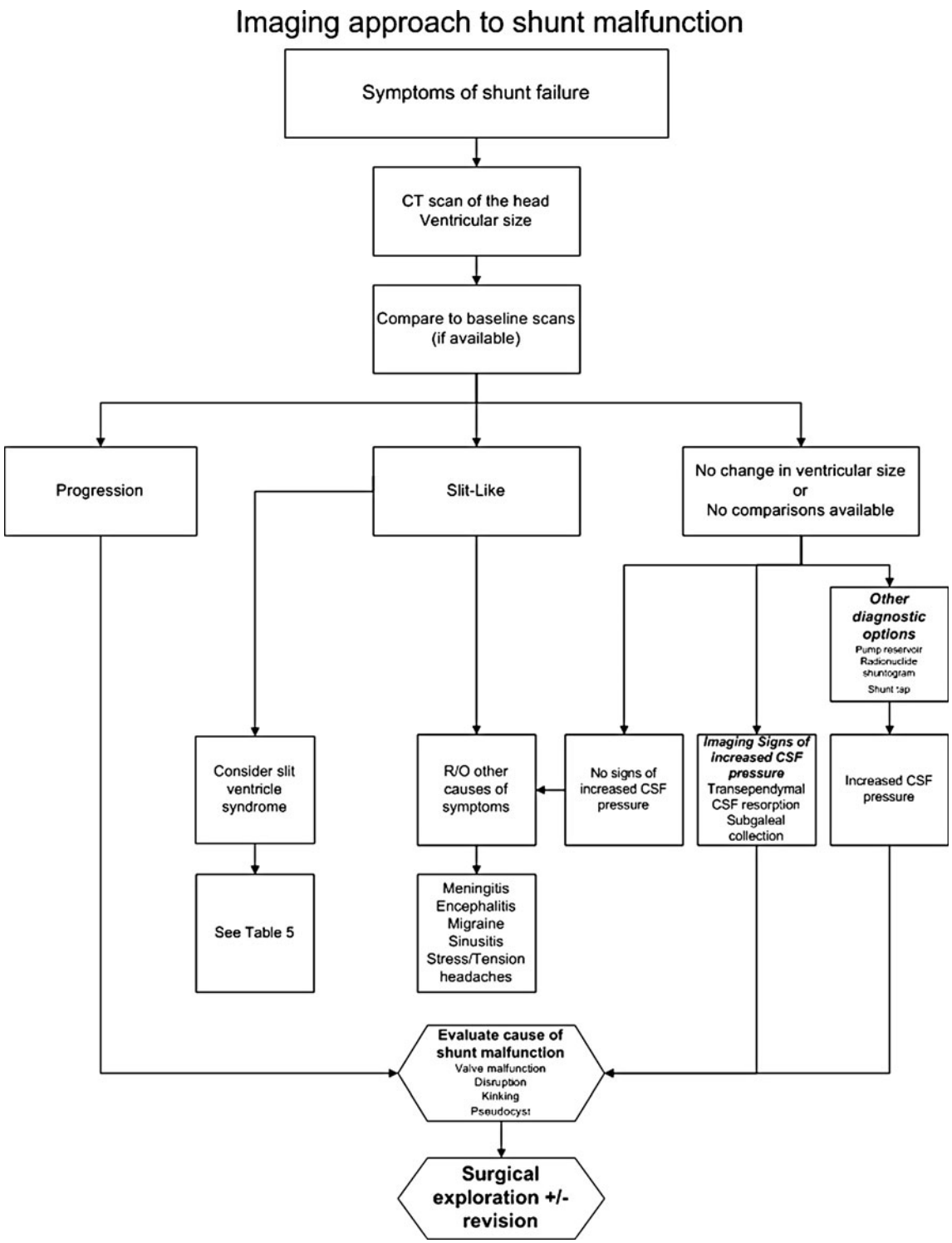

Fig. 23 Imaging approach to shunt malfunction (flowchart). Comparison should be made to a prior baseline study and not to a prior study that was obtained when the child was symptomatic

ependymal lining of the ventricles (Fig. 22). It is important to remember that meningeal enhancement is a frequent occurrence in postoperative patients and is not a sign of infection. In terms of treatment, the definitive intervention for infection involves shunt removal in conjunction with systemic and intrashunt antibiotic

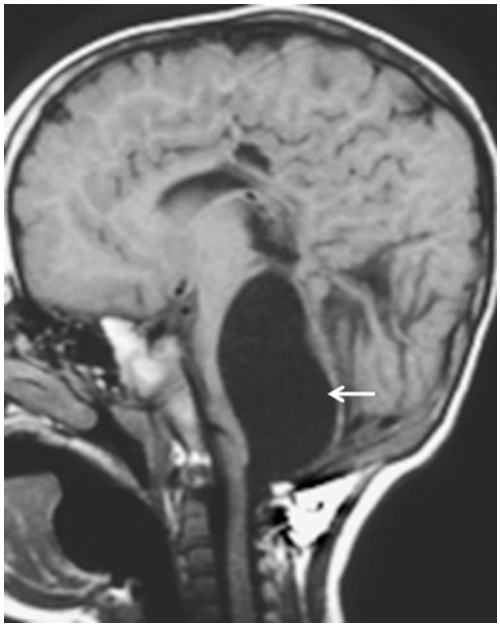

Fig. 24 Sagittal MR reveals cystic fourth ventricular dilatation due to outlet obstruction (*arrow*)

therapy. A temporary external drain is placed for drainage and monitoring CSF cultures, and a new shunt is inserted after the infection has cleared.

Flowchart

The radiological diagnosis of shunt malfunction revolves around an accurate assessment of the ventricular size, especially on serial studies. As illustrated above, the size of the ventricles may be small, normal or enlarged in the presence of shunt malfunction. The initial assessment based on clinical data, in conjunction with CT findings, leads to decisions regarding further evaluation as illustrated in Fig. 23.

Chronic sequelae of shunt placement

Trapped fourth ventricle

Repeated hemorrhage or infection may lead to scarring of the cerebral aqueduct and the foramina of Magendie and Luschka, resulting in a trapped fourth ventricle. The trapped ventricle may attain large proportions and become a cause of obstructive hydrocephalus. In shunted children, this phenomenon is quite rare with an estimated incidence of 2.4% to 3.0% [45]. The multiplanar capability of MRI is useful in this situation as it provides a view of the cerebral aqueduct (Fig. 24). Symptomatic children can be treated with a second catheter to drain the fourth ventricle.

Isolated lateral ventricle and intracranial cysts

Asymmetry in the size of the lateral ventricles or isolated pockets of CSF (loculations) in a periventricular distribution is a frequent finding in chronically shunted patients (Fig. 25). The majority of loculations are postinfectious or postinflammatory, but CSF overdrainage can also be a cause. MRI is often useful for delineating complex ventricular anatomy in these cases. Obstruction of a portion of the lateral ventricle, with decompression of the rest of the ventricular system, may be diagnosed by the presence of isolated CSF edema around the trapped locule. Diagnosis is also generally possible via an iohexol intraventricular dye study. Once the dye is injected into the ventricular system, it diffuses into all areas except any locules, or becomes sequestered within a specific locule [46]. Treatment is possible

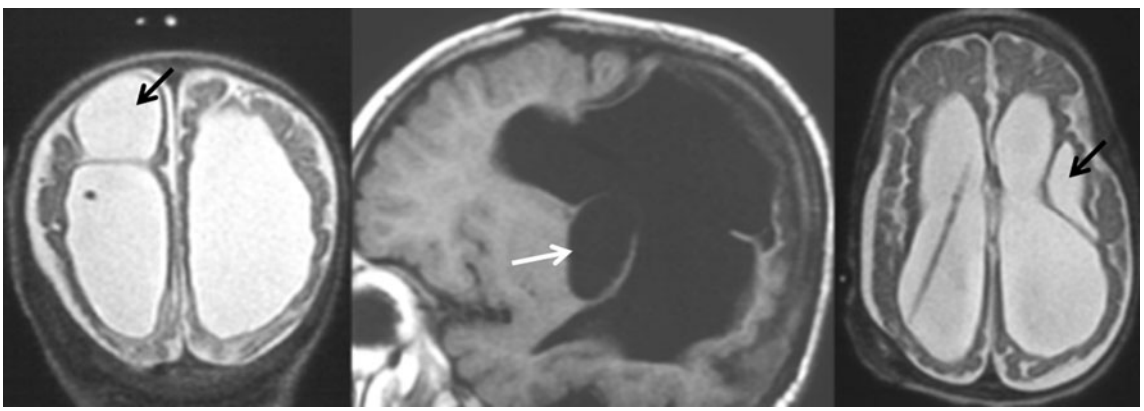

Fig. 25 MRI with loculated fluid. Left image: Hydrocephalus with CSF loculation extending superiorly from the right lateral ventricle (*black arrow*). Middle and right images: Hydrocephalus with multiple complex CSF loculations seen on the sagittal and axial images

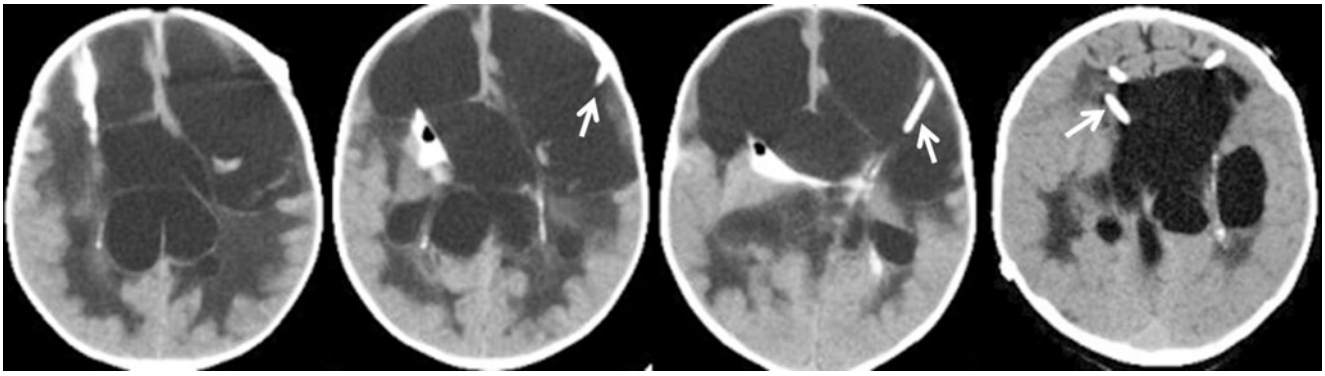

Fig. 26 Axial CT images show multiple proximal shunt catheters (*arrows*) deployed for the drainage of complex loculated hydrocephalus

by endoscopic cyst fenestration under neuroimaging guidance (US or MRI), which reestablishes communications between the loculations, with subsequent drainage by a single ventricular catheter. In complex cases, the use of multiple shunt catheters is inevitable. Determining the function of each of these catheters at follow-up imaging can be a major challenge (Fig. 26).

Subdural fluid collections

In children with fixed head size, subdural fluid collections can occur as a result of the disparity between brain size and head size following shunting. One source attributes subdural fluid collections to subarachnoid or arachnoid vessel disruption [25]. These children are usually asymptomatic, and the condition resolves with brain growth. However, severe subdural collections secondary to overdrainage may benefit from changing the valve or adding a drainage-limiting device (Fig. 27). Symptomatic children may require subdural catheter placement with connection of the catheter to the shunt.

Other sequelae

Chronic overdrainage of CSF can result in premature closure of cranial sutures, or craniosynostosis, which occurs in 1–5.4% of children with shunts [47]. This condition is caused by the failure of a decompressed and compliant brain to exert the requisite mechanical pressure on the growing skull bones to keep sutures open. In these situations, a craniectomy may be required to allow for future brain growth (Fig. 28). Another finding is meningeal fibrosis, which may be seen as a result of chronic subdural fluid collections. Collagen and vascular granulation tissue accumulate, resulting in intense enhancement on MRI or CT with contrast agent. Peri-shunt encephalomalacia and periventricular leukomalacia are also commonly seen in chronically shunted patients. Moreover, there are the ever-present risks of peritoneal adhesions, ascites and peritonitis. The presence of these more complicated sequelae may necessitate the use of ventriculopleural shunts. These shunts are not first-line options for the treatment of hydrocephalus due to the risk of respiratory insufficiency secondary to pneumothorax or pleural effusion.

Conclusion

There is no consensus regarding the most cost-efficient means of evaluating suspected shunt malfunction. In most centers, a complete battery of tests is ordered when a child with suspected shunt malfunction enters the emergency room. We know, however, that initial triage using clinical examination and a CT scan of the head considerably narrows the differential diagnosis. This approach allows a

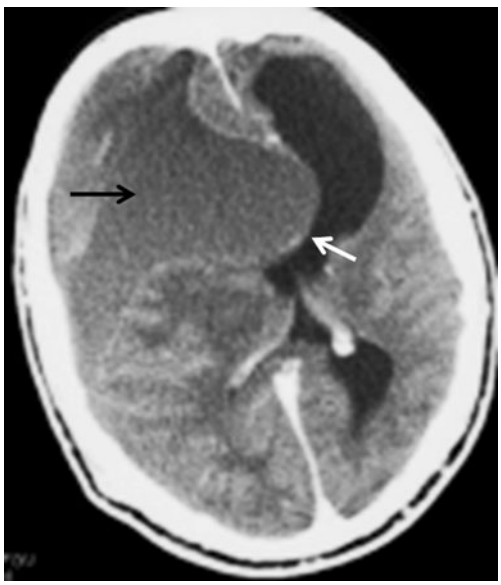

Fig. 27 Axial CT shows right-side cortical mantle collapse (*white arrow*) and subacute subdural hematoma (*black arrow*) resulting from overdrainage

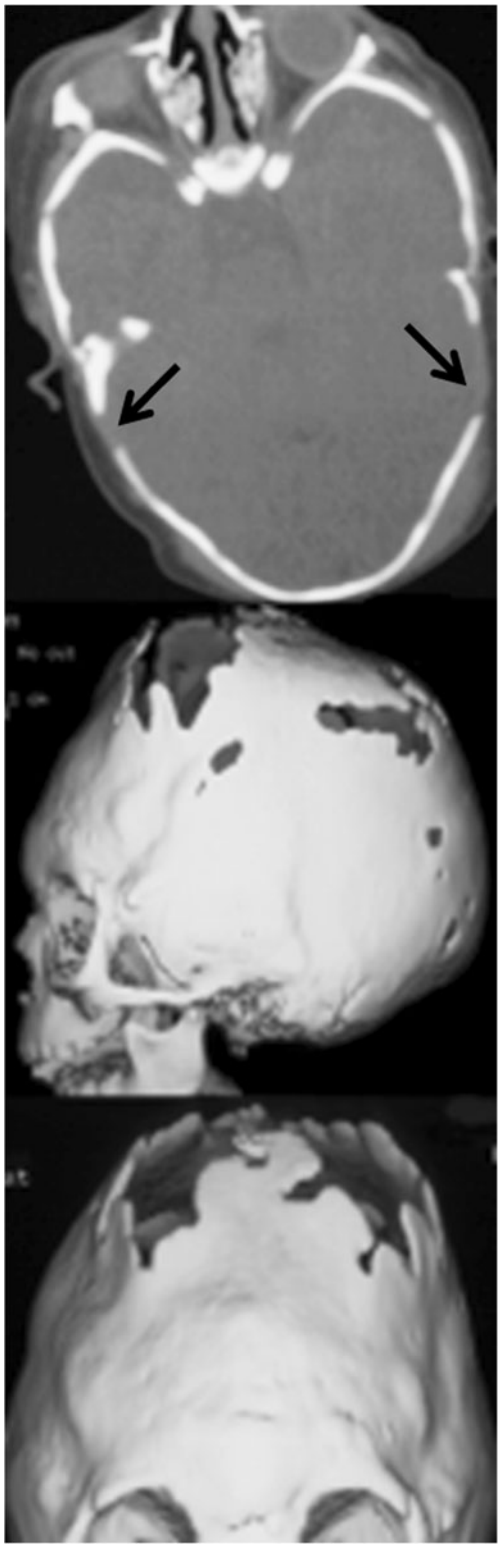

Fig. 28 Axial and 3D CT images show cranial vault decompression (*arrows*) and remodeling for craniosynostosis that developed from chronic CSF shunting

decision regarding shunt revision to be made, and leads to definitive localization of the site of shunt malfunction. However, much remains to be investigated. What is the most cost-effective means of diagnosing shunt malfunction? In this current economic climate, issues of cost to the patient must be factored in to these decisions. Will there be specific guidelines for radiology in surveillance of shunts to prevent shunt malfunction? What will be the future role of methods such as low-dose CT and radiation-free "rapid MRI," and will they usher in other methods that minimize risks to the child while maximizing diagnostic value? Questions such as these await well-planned prospective studies or new tools of diagnosis.

Acknowledgments We would like to acknowledge the assistance of Mrs. Shireen Hayatghaibi in creating the flowchart in Figure 23 using Microsoft Visio software, and the assistance of Dr. Serife Kavuk in the preparation of the images.

References

1. Wu Y, Green NL, Wrensch MR et al (2007) Ventriculoperitoneal shunt complications in California: 1990 to 2000. Neurosurgery 61:557–562
2. Patwardhan RV, Nanda A (2005) Implanted ventricular shunts in the United States: the billion-dollar-a-year cost of hydrocephalus treatment. Neurosurgery 56:139–145
3. Olson S (2004) The problematic slit ventricle syndrome. A review of the literature and proposed algorithm for treatment. Pediatr Neurosurg 40:264–269
4. Browd SR, Ragel BT, Gottfried ON et al (2006) Failure of cerebrospinal fluid shunts: part I: obstruction and mechanical failure. Pediatr Neurol 34:83–92
5. Drake JM (1993) Ventriculostomy for treatment of hydrocephalus. Neurosurg Clin N Am 4:657–666
6. Hopf NJ, Grunert P, Fries G et al (1999) Endoscopic third ventriculostomy: outcome analysis of 100 consecutive procedures. Neurosurgery 44:795–804 discussion 804–806
7. Dias MS, Li V (1998) Pediatric neurosurgical disease. Pediatr Clin N Am 45:1539–1578
8. Khorasani L, Sikorski CW, Frim DM (2004) Lumbar CSF shunting preferentially drains the cerebral subarachnoid over the ventricular spaces: implications for the treatment of slit ventricle syndrome. Pediatr Neurosurg 40:270–276
9. Yadav YR, Pande S, Raina VK et al (2004) Lumboperitoneal shunts: review of 409 cases. Neurol India 52:188–190
10. Lollis SS, Mamourian AC, Vaccaro TJ et al (2010) Programmable CSF shunt valves: radiographic identification and interpretation. AJNR 31:1343–1346
11. Eastwood S (ed) (1986) About hydrocephalus. A book for parents. The Hydrocephalus Association and the University of California at San Francisco
12. Mataro M, Poca MA, Sahuquillo J et al (2000) Cognitive changes after cerebrospinal fluid shunting in young adults with spina bifida and assumed arrested hydrocephalus. J Neurol Neurosurg Psychiatry 68:615–621
13. McGirt MJ, Leveque JC, Wellons JC 3rd et al (2002) Cerebrospinal fluid shunt survival and etiology of failures: a seven-year institutional experience. Pediatr Neurosurg 36:248–255

14. Tuli S, Drake J, Lawless J et al (2000) Risk factors for repeated cerebrospinal shunt failures in pediatric patients with hydrocephalus. J Neurosurg 92:31–38
15. Garton HJ, Kestle JR, Drake JM (2001) Predicting shunt failure from clinical symptoms and signs. J Neurosurg 94:202–210
16. Li V, Dias MS (1999) The results of a practice survey on the management of patients with shunted hydrocephalus. Pediatr Neurosurg 30:288–295
17. Ramamurthi R (2005) Textbook of operative neurosurgery. B.I. Publications, New Delhi
18. Udayansankar UK, Braithwaite K, Arvaniti M et al (2008) Low-dose nonenhanced head CT protocol for follow-up evaluation of children with ventriculoperitoneal shunt: reduction of radiation and effect on image quality. AJNR 29:802–806
19. Desai KR, Babb JS, Amodio JB (2007) The utility of the plain radiograph "shunt series" in the evaluation of suspected ventriculoperitoneal shunt failure in pediatric patients. Pediatr Radiol 37:452–456
20. Ouellette D, Lynch T, Bruder E et al (2009) Additive value of nuclear medicine shuntograms to computed tomography for suspected cerebrospinal fluid shunt obstruction in the pediatric emergency department. Pediatr Emerg Care 25:827–830
21. Kurwale NS, Agrawal D (2010) Phase contrast MRI of intracranial shunt tube: a valuable adjunct in the diagnosis of ventriculoperitoneal shunt malfunction. Neurosurgery 67:552–553
22. Iskander BJ, Sansone JM, Medow J et al (2004) The use of quick-brain magnetic resonance imaging in the evaluation of shunt-treated hydrocephalus. J Neurosurg Pediatr 101:147–151
23. Collins P, Hockley AD, Woollam DH (1978) Surface ultrastructure of tissues occluding ventricular catheters. J Neurosurg 48:609–613
24. Kast J, Duong D, Nowzari F et al (1994) Time-related patterns of ventricular shunt failure. Childs Nerv Syst 10:524–528
25. Drake JM, Sainte-Rose C (1995) Shunt complications. In: Drake JM, Sainte-Rose C (eds) The shunt book. Blackwell, Cambridge
26. Piatt JH Jr (1996) Pumping the shunt revisited: a longitudinal study. Pediatr Neurosurg 25:73–76
27. Uvebrant P, Sixt R, Bjure J et al (1992) Evaluation of cerebrospinal fluid shunt function in hydrocephalic children using 99mTc-DTPA. Childs Nerv Syst 8:76–80
28. May CH, Aurisch R, Kornrumpf D et al (1999) Evaluation of shunt function in hydrocephalic patients with the radionuclide 99mTc-pertechnetate. Childs Nerv Syst 15:239–424 discussion 245
29. O'Brien DF, Taylor M, Park TS et al (2003) A critical analysis of 'normal' radionucleotide shuntograms in patients subsequently requiring surgery. Childs Nerv Syst 19:337–341
30. Buxton N, Punt J (1999) Subtemporal decompression: the treatment of noncompliant ventricle syndrome. Neurosurgery 44:513–519
31. Obana WG, Raskin NH et al (1990) Antimigraine treatment for slit ventricle syndrome. Neurosurgery 27:760–763
32. Linder M, Diehl J, Sklar FH (1983) Subtemporal decompressions for shunt dependent ventricles: mechanism of action. Surg Neurol 19:520–525
33. Di Rocco C, Marchese E, Velardi F (1994) A survey of the first complication of newly implanted CSF shunt devices for the treatment of nontumoral hydrocephalus. Cooperative survey of the 1991–1992 Education Committee on the ISPN. Childs Nerv Syst 10:321–327
34. Kestle J, Drake J, Milner R et al (2000) Long-term follow-up data from the Shunt Design Trial. Pediatr Neurosurg 33:230–236
35. Vernet O, Campiche R, de Tribolet N (1995) Long-term results after ventriculo-atrial shunting in children. Childs Nerv Syst 11:176–179
36. Major O, Fedorcsak I, Sipos L et al (1994) Slit-ventricle syndrome in shunt operated children. Acta Neurochir 127:69–72
37. Sgouros S, Malluci C, Walsh AR et al (1995) Long-term complications of hydrocephalus. Pediatr Neurosurg 23:127–132
38. Epstein F, Lapras C, Wisoff JH (1988) 'Slit ventricle syndrome': etiology and treatment. Pediatr Neurosci 14:5–10
39. Holness RO, Hoffman HJ, Hendrick EB (1979) Subtemporal decompression for the slit ventricle syndrome after shunting in hydrocephalic children. Childs Brain 5:137–144
40. Eldredge EA, Rockoff MA, Medlock MD et al (1997) Postoperative cerebral edema occurring in children with slit ventricles. Pediatrics 99:625–630
41. Ghotme K, Drake J, Lamberti-Pasculli M et al (2007) Management of shunt disconnections and fractures in children: experience at the Hospital for Sick Children. AANS Pediatric Section Meeting, South Beach, FL
42. Storrow AB (1998) Intracranial shunt assessment. In: Hedges JR (ed) Clinical procedures in emergency medicine, 3rd edn. Saunders, Philadelphia
43. Nelson JD (1984) Cerebrospinal fluid shunt infections. Pediatr Infect Dis 3:S30–S32
44. Tunkel AR, Scheld WM (2000) Acute meningitis. In: Mandell GL, Bennett JE, Dolin R (eds) Principles and practice of infectious diseases. Churchill Livingstone, Philadelphia
45. Upchurch K, Raifu M, Bergsneider M (2007) Endoscope-assisted placement of a multiperforated shunt catheter into the fourth ventricle via a frontal transventricular approach. Neurosurg Focus 22:1–8
46. Browd SR, Ragel BT, Gottfried ON et al (2006) Failure of cerebrospinal fluid shunts: part II: overdrainage, loculation, and abdominal complications. Pediatr Neurol 34:171–176
47. Park DH, Chung J, Yoon SH (2009) The role of distraction osteogenesis in children with secondary craniosynostosis after shunt operation in early infancy. Pediatr Neurosurg 45:437–445